

ACCURACY ANALYSIS ON LARGE BLOCKS OF HIGH RESOLUTION IMAGES

Dr. Ing. Ricardo M. Passini
BAE SYSTEMS ADR



- **INTRODUCTION**
- **SHORT DESCRIPTION OF THE ORIENTATION MODELS**
- **EXPERIMENTAL TESTS**
- **ANALYSIS OF THE RESULTS**
- **CONCLUSIONS**
- **RECOMMENDATIONS**

***“TODAY EXISTING HIGH RESOLUTION
IMAGES ARE ENTERING INTO
COMPETITION WITH AERIAL
PHOTOGRAPHY FOR REGIONAL
MAPPING PROGRAMS AND OTHER
EXTENSIVE MAPPING APPLICATIONS
WHERE HIGH RESOLUTION IS
REQUIRED”***

***OUR STUDY IS CONCENTRATED MAINLY ON
QUICKBIRD IMAGES***

USE OF VERY HIGH RESOLUTION IMAGES

Mapping, Risk Management, Forest, Geology, Regional Planning, Utility Corridor Planning, Mapping for E911 applications, Defense Mapping, etc.

1. Information contents

Rule of thumb: for **topographic maps** **0.05 – 0.1 mm pixel size in map** required

based on 1m pixel size → map **1 : 10 000** (~ 1"=800')

based on 0,6m pixel size → map **1 : 6000** (1"=500')

For **orthoimages** **8 pixel / mm (0.125 m pixel size)**

based on 1m pixel size → orthoimage **1 : 8000** (~1"=667')

based on 0,6m pixel size → orthoimage **1 : 4800** (1"=400')

2. Accuracy

Required accuracy of x, y- coordinates: ~ 0,25mm in map, in orthoimage ~ 0,3mm

→ **required ground accuracy 2,5m / 1,5m (0.25 mm at above map scales)**

Image orientation must be better because of additional error components

ACCURACY DEPENDS ON:

- **Orientation Model used**
- **GCPs (Number, Distribution, Geometric & Radiometric Quality, etc.)**
- **For Orthos (DTM accuracy, Resolution, Fidelity of Terrain Reconstruction, etc)**
- **Others**

USED ORIENTATION MODELS IN THE INVESTIGATION:

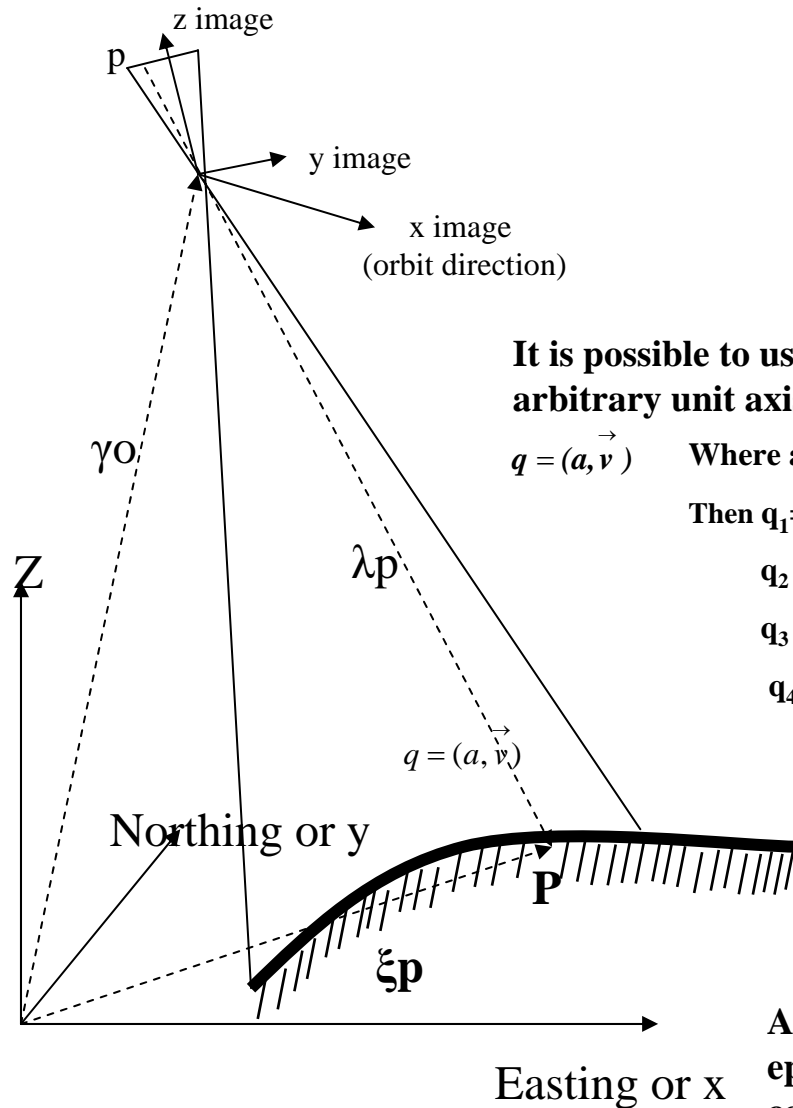
- **SIMULTANEOUS BUNDLE BLOCK ADJUSTMENT (using ephemeris & quaternion algebra)**
- **RATIONAL POLINOMIAL COEFFICIENTS (+image correction functions)**

USED IMAGE:

- **A block of 40 QB Basic images with limited overlap (hilly, equatorial, jungle zone)**

GROUND CONTROL:

Manually Transferred from existing oriented aerial photography (1:20,000)



$$\xi p = \gamma o + \lambda p \quad \text{or}$$

$$0 = -c \frac{a_{11}^j (Xp - Xo^j) + a_{12}^j (Yp - Yo^j) + a_{13}^j (Zp - Zo^j)}{a_{31}^j (Xp - Xo^j) + a_{32}^j (Yp - Yo^j) + a_{33}^j (Zp - Zo^j)}$$

$$y = \frac{-c \frac{a_{21}^j (Xp - Xo^j) + a_{22}^j (Yp - Yo^j) + a_{23}^j (Zp - Zo^j)}{a_{31}^j (Xp - Xo^j) + a_{32}^j (Yp - Yo^j) + a_{33}^j (Zp - Zo^j)}}{1}$$

It is possible to use quaternion multiplication to perform a rotation about an arbitrary unit axis \mathbf{m} by an angle Θ . The quaternion that computes the rotation is:

$$q = (a, \vec{v}) \quad \text{Where } a = \cos(\Theta/2), v = \sin(\Theta/2).$$

Then $q_1 = \mu_x \sin(\Theta/2)$,

$$q_2 = \mu_y \sin(\Theta/2)$$

$$\mathbf{q}_3 = \mu_z \sin(\Theta/2)$$

$$\mathbf{q}_4 = \cos(\Theta/2)$$

A point in 3D $p = (0, \vec{P})$ $q = a + bi + cj + dk$

is rotated by $\mathbf{P}_{rotated} = \mathbf{q} * \mathbf{p} * \mathbf{q}^{-1}$

The orthogonal rotation matrix corresponding to a rotation by the unit quaternion $p=a+bi+cj+dk$ is given by $q^*q^{-1} =$

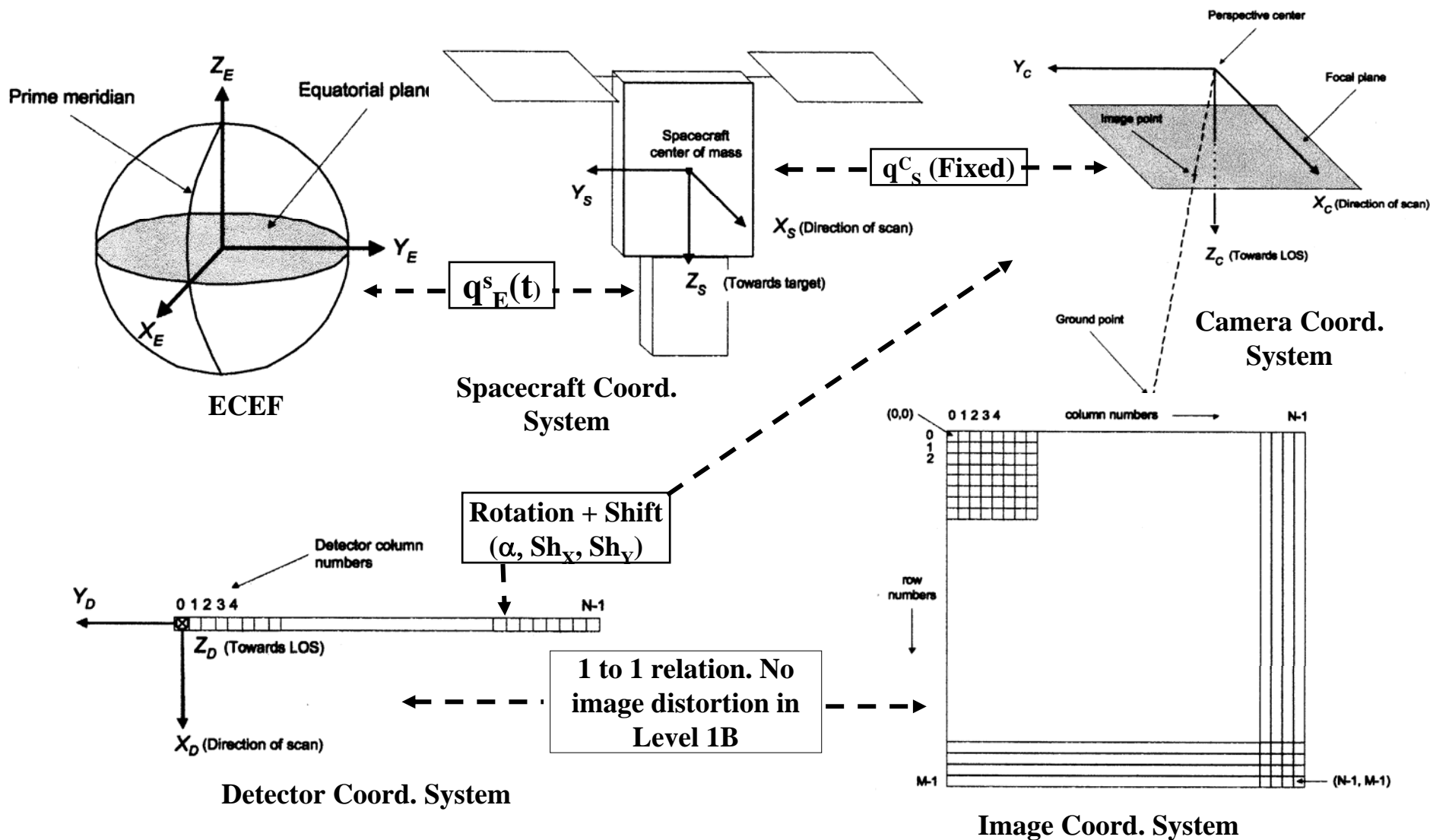
$$\mathbf{q}^* \mathbf{q}^{-1} = \begin{pmatrix} a^2 + b^2 - c^2 - d^2 & 2bc - 2ad & 2ac + 2bd \\ 2ad + 2bc & a^2 - b^2 + c^2 - d^2 & 2cd - 2ab \\ 2bd - 2ac & 2ab + 2cd & a^2 - b^2 - c^2 + d^2 \end{pmatrix}$$

Assuming smooth stable paths (that generally is), then no ephemeris corrections are applied, only attitude corrections are computed in the adjustment.

Bundle Orientation using ephemeris and quaternion algebra

The QB Camera Sensor Model includes the Coordinate Systems:

BAE SYSTEMS



Bundle Orientation using ephemeris and quaternion algebra

Derivation of the co-linearity equations

As the Level 1B product is sampled at a constant rate, the corresponding time (t)= $t=r/\text{avgLineRate} + \text{firstLineTime}$

One point on the imaging ray is the perspective centre of the virtual camera at time t. The coordinates of the perspective centre in the spacecraft coordinate systems are constant and given data. In matrix notation: $C_S = (CX, CY, CZ)^T$ (from *.geo file)

It is possible to locate the origin of the spacecraft coordinate system in the ECF system at a time t by interpolating the position time series in the ephemeris file. Let us call this position $S_E(t)$. Likewise, we can find the attitude of the spacecraft coordinate system at a time (t) in the ECF system by interpolating the quaternion time series in the attitude file. This quaternion, $q_E^S(t)$, represents the rotation from the ECF system to the spacecraft body system at time t. Then using quaternion algebra, the position of the perspective centre at time t in the ECF coordinate system is:

$$C_E(t) = (q_E^S(t))^{-1} C_S q_E^S(t) + S_E(t), \text{ or}$$

$$C_E(t) = q_E^S(t) C_S (q_E^S(t))^{-1} + S_E(t) \text{ or } CE(t) = R_E^S(t) C_S + S_E(t) \text{ This is the Projection Center if ECEF}$$

Any point that we measure (c,r) is expressed in the detector system as

$$XD=0, \quad YD=-c*\text{detPitch} \text{ (detPitch: Calibrated distance between pixels)}$$

In the camera system is

$$X_C = \cos(\alpha)* XD - \sin(\alpha)* YD + Sh_X;$$

$$Y_C = \sin(\alpha)* XD + \cos(\alpha)* YD + Sh_Y; Z_C = C \text{ (Nominal Principal Distance)}$$

As Level 1B images do not have lens distortion the image point is identical to the measured image point, hence: $X_C=X_C, Y_C=Y_C, Z_C=Z_C$.

The unit vector wC that is parallel to the external ray in the camera coordinate system is just the position of (XC', YC', ZC') relative to the perspective centre at (0, 0, 0), normalized by its length. In matrix notation, this vector is: $W_C = (X_C, Y_C, Z_C)^T$ & $w_C = W_C / \|W_C\|$

It is possible to convert this vector first to the spacecraft coordinate system and then to the ECF system. The unit quaternion for the attitude of the camera coordinate system, i.e., the quaternion for the rotation of spacecraft frame into the camera frame q_S^C , is in the geometric calibration file (*.geo). Then, using quaternion algebra:

$$w_E = q_E^S(t)^{-1} q_S^C^{-1} w_C q_S^C q_E^S(t) \text{ or } w_E = q_E^S(t) q_S^C w_C (q_E^S(t) q_S^C)^{-1} \text{ or using matrix algebra, } w_E = R_E^S(t) R_S^C w_C$$

Hence, the co-linearity equation will be:

$$w_C = [R_E^S(t) R_S^C] \text{ or } w_C = (q_E^S(t) q_S^C)^{-1} w_E [q_E^S(t) q_S^C]^T$$

Bundle Orientation using ephemeris and quaternion algebra

Ephemeris and Quaternion data. Variance-Co-variance Matrix

- **Ephemeris File:** Sample mean and covariance estimates of the position of the spacecraft system relative to the ECEF system. These data are produced for a continuous image period, e.g., an image strip, and spans the period from at least 4 seconds before start of imaging to at least four seconds after the end of imaging
- **Attitude File:** Contains Sample mean and covariance estimates of the attitude of the spacecraft system relative to the ECEF system. These data are also produced for a continuous image period, e.g., an image strip, and spans the period from at least 4 seconds before start of imaging to at least four seconds after the end of imaging
- **Sampling rate** (timeInterval): Each 0.02 seconds. For intermediate position only linear interpolation is required
- **Possibility to implement a weighting schema based on:**

$$\begin{array}{ccc} \sigma X_o^2 & \sigma X_o Y_o & \sigma X_o Z_o \\ & \sigma Y_o^2 & \sigma Y_o Z_o \\ & & \sigma Z_o^2 \end{array}$$

$$\begin{array}{cccc} \sigma q_1^2 & \sigma q_1 q_2 & \sigma q_1 q_3 & \sigma q_1 q_4 \\ & \sigma q_2^2 & \sigma q_2 q_3 & \sigma q_2 q_4 \\ & & \sigma q_3^2 & \sigma q_3 q_4 \\ & & & \sigma q_4^2 \end{array}$$

{Image Space (Line, Sample)} *FUNCTIONAL RELATION* {Object Space (ϕ, λ, h)}

$$P = \frac{\phi - LAT_OFF}{LAT_SCALE} \quad L = \frac{\lambda - LONG_OFF}{LONG_SCALE} \quad H = \frac{h - HEIGHT_OFF}{HEIGHT_SCALE}$$

$$y = Line = g(\phi, \lambda, h) = \frac{NUM_L(P, L, H)}{DEN_L(P, L, H)} = \frac{a^T A}{b^T B} \quad x = Sample = h(\phi, \lambda, h) = \frac{NUM_S(P, L, H)}{DEN_S(P, L, H)} = \frac{c^T A}{d^T A}$$

$$NUM_L(P, L, H) = a_1 + a_2 L + a_3 P + a_4 H + a_5 LP + a_6 LH + a_7 PH + a_8 L^2 + a_9 P^2 + a_{10} H^2 + a_{11} PLH + a_{12} L^3 + a_{13} LP^2 + a_{14} LH^2 + a_{15} L^2 P + a_{16} P^3 + a_{17} PH^2 + a_{18} L^2 H + a_{19} P^2 H + a_{20} H^3 = a^T A$$

$$DEN_L(P, L, H) = b_1 + b_2 L + b_3 P + b_4 H + b_5 LP + b_6 LH + b_7 PH + b_8 L^2 + b_9 P^2 + b_{10} H^2 + b_{11} PLH + b_{12} L^3 + b_{13} LP^2 + b_{14} LH^2 + b_{15} L^2 P + b_{16} P^3 + b_{17} PH^2 + b_{18} L^2 H + b_{19} P^2 H + b_{20} H^3 = b^T A$$

The de-normalized image space coordinates (*Line, Sample*), can also be computed from:

$$Line = y. LINE_SCALE + LINE_OFF \quad Sample = x. SAMP_SCALE + SAMP_OFF$$

Computed de-normalized image coordinates (*Line, Sample*)

≠ Observed image Coordinates (*Line, Sample*)

$$\mathbf{Line}_i^{(j)} = \xi^{(j)}(\varphi_s, \lambda_s, h_s) + d\xi^{(j)} + \nabla_{Li} \quad \mathbf{Sample}_i^{(j)} = \rho^{(j)}(\varphi_s, \lambda_s, h_s) + d\rho^{(j)} + \nabla_{Si}$$

With: $\mathbf{Line}_i^{(j)}$ and $\mathbf{Sample}_i^{(j)}$ measured image coordinates of a TP or GCP s with coordinates $(\varphi_s, \lambda_s, h_s)$

$\xi^{(j)}(\varphi_s, \lambda_s, h_s)$ and $\rho^{(j)}(\varphi_s, \lambda_s, h_s)$ computed de-normalized image coordinates of the GCP or tie point s

$d\xi^{(j)}$ and $d\rho^{(j)}$ Correction Functions to account for the difference between measured and computed coordinates

∇_{Li} and ∇_{Si} are random errors. Or:

$$\xi^{(j)}(\varphi_s, \lambda_s, h_s) = g(\varphi, \lambda, h) \cdot \text{LINE_SCALE} + \text{LINE_OFF} \quad \rho^{(j)}(\varphi_s, \lambda_s, h_s) = h(\varphi, \lambda, h) \cdot \text{SAMPLE_SCALE} + \text{SAMPLE_OFF}$$

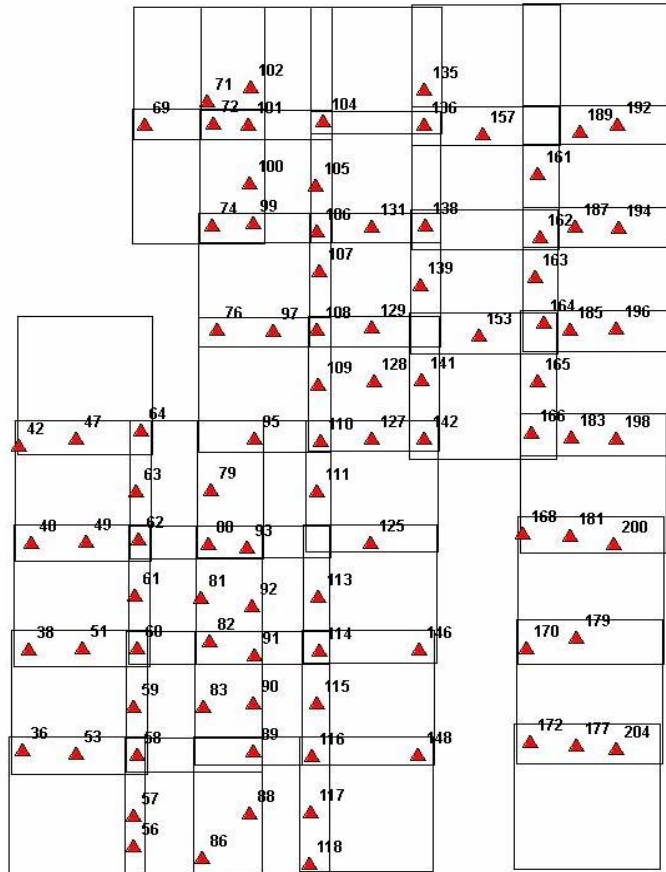
$$d\xi = r_o + r_s \cdot \overline{\mathbf{Sample}} + r_L \cdot \overline{\mathbf{Line}} \quad d\rho = s_o + s_s \cdot \overline{\mathbf{Sample}} + s_L \cdot \overline{\mathbf{Line}}$$

$$\varphi_{Li_o} + \frac{\partial \varphi_{Li}}{\partial r_o^{(j)}} dr_o^{(j)} + \frac{\partial \varphi_{Li}}{\partial r_s^{(j)}} dr_s^{(j)} + \frac{\partial \varphi_{Li}}{\partial r_L^{(j)}} dr_L^{(j)} + \frac{\partial \varphi_{Li}}{\partial \varphi_s} d\varphi_s + \frac{\partial \varphi_{Li}}{\partial \lambda_s} d\lambda_s + \frac{\partial \varphi_{Li}}{\partial h_s} dh_s = v_{Li}^{(j)}$$

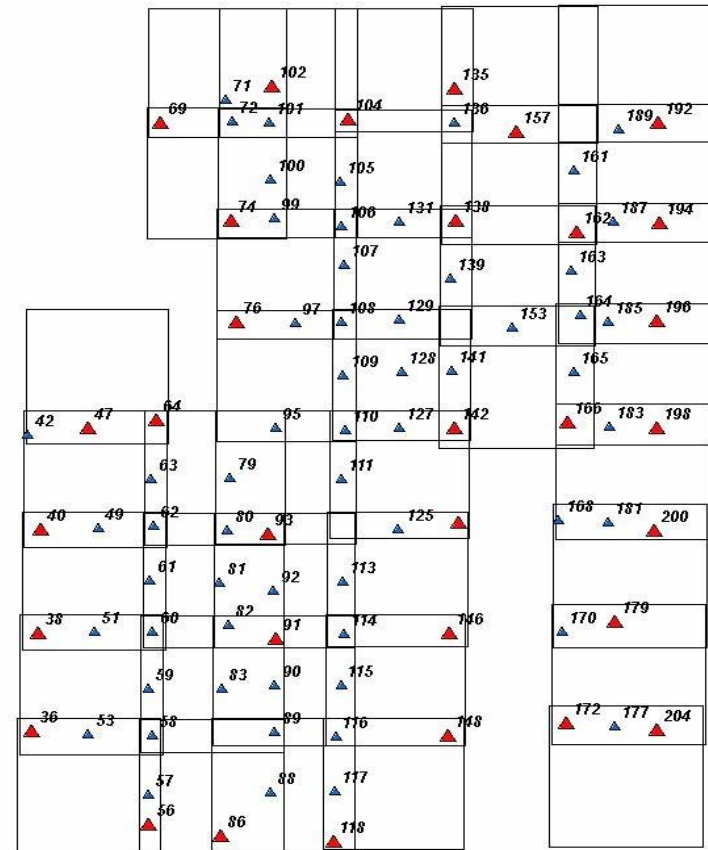
$$\varphi_{Si_o} + \frac{\partial \varphi_{Si}}{\partial s_o^{(j)}} ds_o^{(j)} + \frac{\partial \varphi_{Si}}{\partial s_s^{(j)}} ds_s^{(j)} + \frac{\partial \varphi_{Si}}{\partial s_L^{(j)}} ds_L^{(j)} + \frac{\partial \varphi_{Si}}{\partial \varphi_s} d\varphi_s + \frac{\partial \varphi_{Si}}{\partial \lambda_s} d\lambda_s + \frac{\partial \varphi_{Si}}{\partial h_s} dh_s = v_{Si}^{(j)}$$

$$\mathbf{X} = (\mathbf{A}^T \mathbf{P} \mathbf{A})^{-1} (\mathbf{A}^T \mathbf{P} \mathbf{L})$$

Experimental Tests. Block of 40 QB Basic images



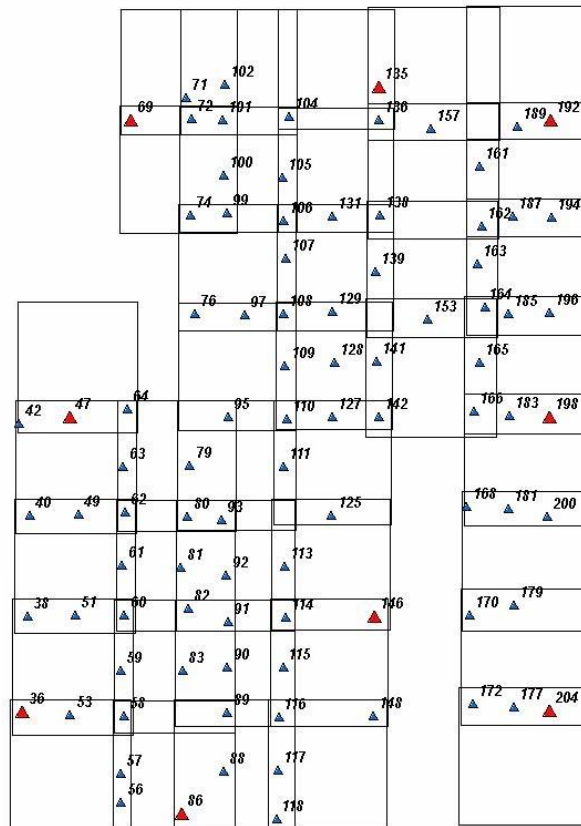
Full Control
Distribution (Case A)



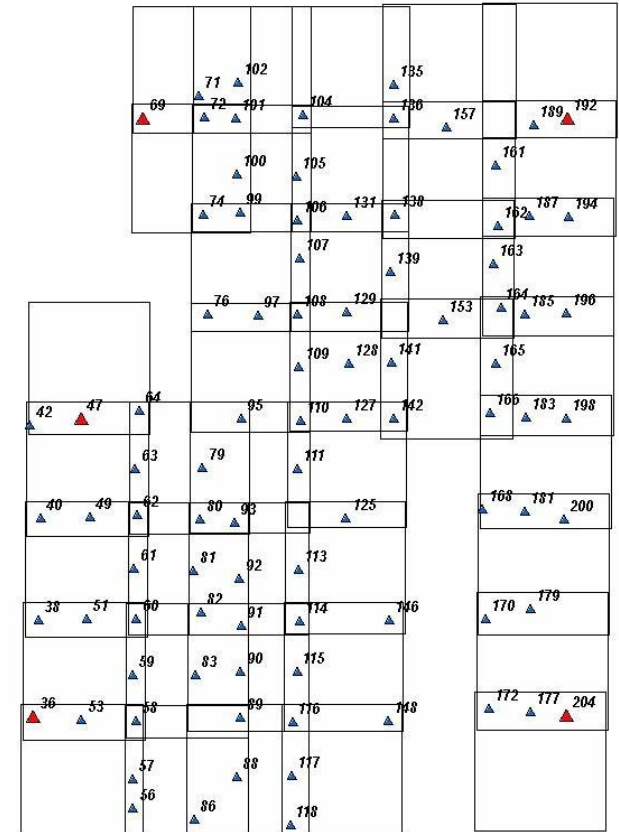
Perimeter Control and randomly distributed GCPs in the center of
the Block. (Case B)

Experimental Tests. Block of 40 QB Basic images

Relaxed perimeter control.
(Case D)



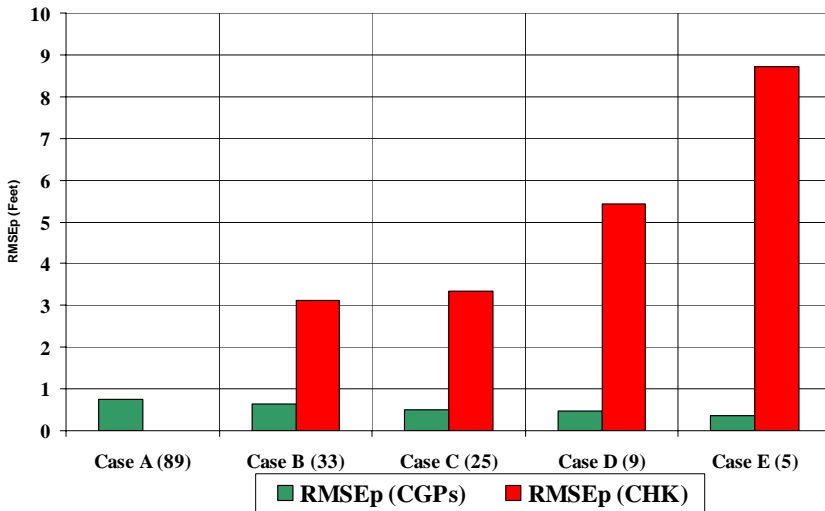
Perimeter control only.
(Case C)



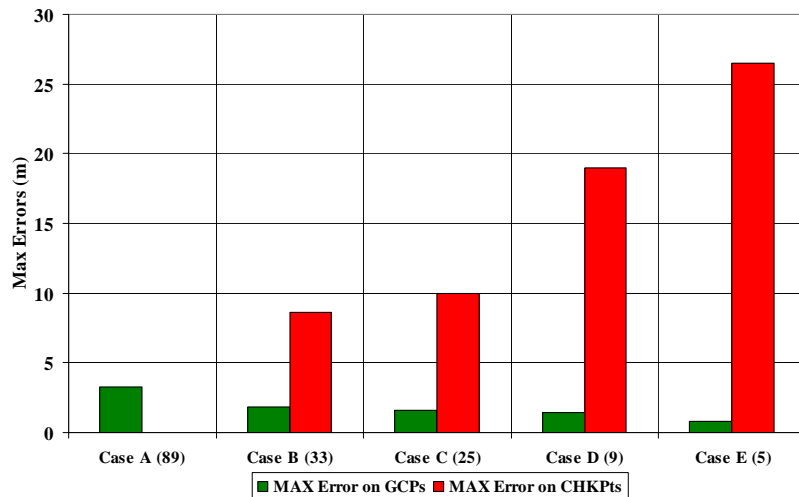
Control only in the corners of the
block. (Case E)

Experimental Tests. Block of 40 QB Basic images

Bundle Adj with Ephemeris & Quaternions



Max Errors on GCPs & CHK Pts



Case	#GCPs	RMSEp	#ChKPts	RMSEp
A	89	0.74		
B	33	0.63	56	3.13
C	25	0.50	64	3.34
D	9	0.47	80	5.42
E	5	0.35	84	8.71

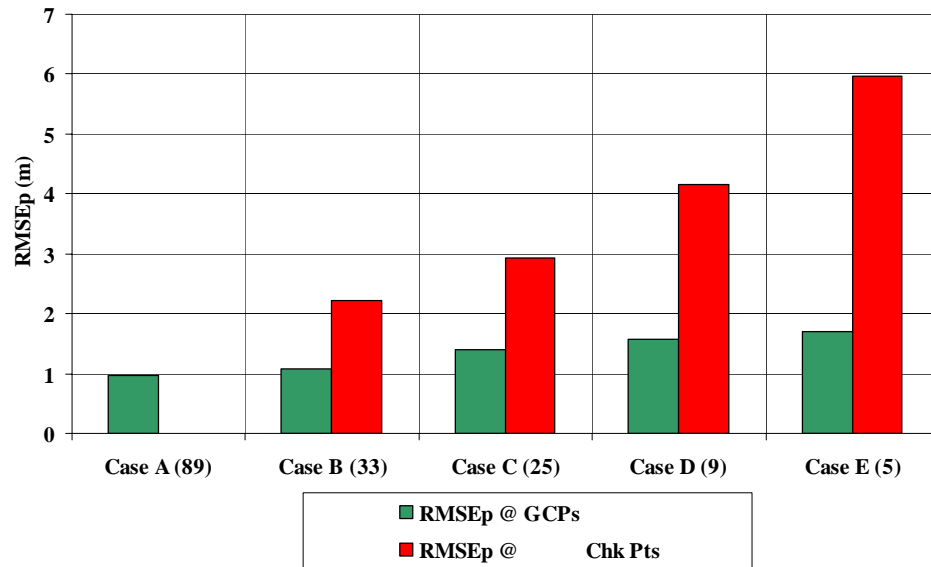
Bundle Adjustment with Ephemeris & Quaternion. Accuracies in GCPs & Check Points

Case	#GCPs	Max Err	#ChKPts	Max Err
A	89	3.27		
B	33	1.87	56	8.61
C	25	1.58	64	10.01
D	9	1.45	80	19.01
E	5	0.81	84	26.49

Bundle Adjustment with Ephemeris & Quaternion. Max Errors on GCPs & Check Points

Experimental Tests. Block of 40 QB Basic images

Block Adj with RPCs + Affine image Correction



Case	#GCPs	RMSEp	#ChKPts	RMSEp
A	89	0.98		
B	33	1.07	56	2.21
C	25	1.41	64	2.93
D	9	1.57	80	4.16
E	5	1.70	84	5.97

Block Adjustment with RPCs + Affine Image Correction

Case	Num GCPs	RMSD [m]		Max Errors [m]	
		Sx	Sy	Δx_{max}	Δy_{max}
A	89	0.21	0.25	2.53	4.93
B	33	0.19	0.23	2.51	4.56
C	25	0.16	0.22	2.48	1.50
D	9	0.16	0.21	2.45	1.48
E	5	0.15	0.20	2.06	1.35

Internal Accuracy. Statistics on TPs. Bundle Adj with Ephemeris & Quaternions

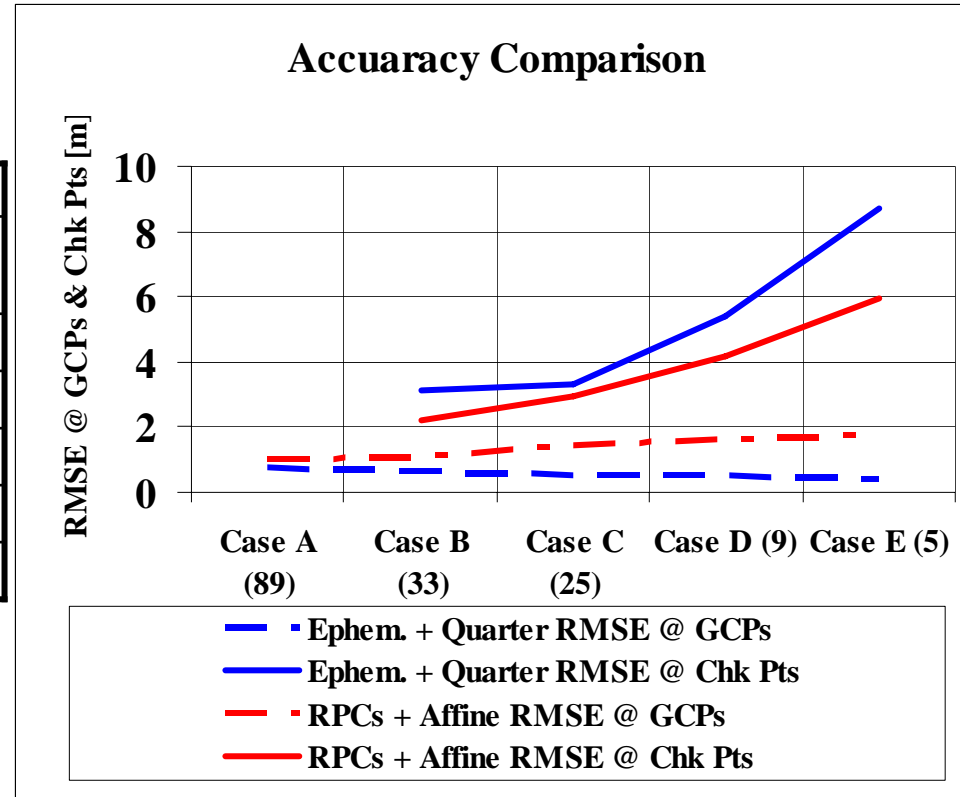
Case	Num GCPs	RMSD [m]		Max Errors [m]	
		Sx	Sy	Δx_{max}	Δy_{max}
A	89	0.29	0.32	1.83	2.57
B	33	0.65	0.74	2.01	3.34
C	25	0.81	0.88	2.49	2.25
D	9	0.88	0.97	2.85	2.98
E	5	0.91	1.12	3.08	3.36

Internal Accuracy. Statistics on TPs. Block Adj with RPCs + Affine Image Correction

Accuracy Comparison. Bundle Adjustment using ephemeris + quaternion vs. Block Adjustment based on RPC and affine image correction

CASE #GCPs	Ephem. + Quarter.		RPCs + Affine	
	RMSE@ GCPs	RMSE@ Chk Pts	RMSE@ GCPs	RMSE@ Chk Pts
A(89)	0.74		0.98	
B(33)	0.63	3.13	1.07	2.21
C(25)	0.50	3.34	1.41	2.93
D(9)	0.47	5.42	1.57	4.16
E(5)	0.35	8.71	1.70	5.97

RMS Errors at GCPs and Check Points

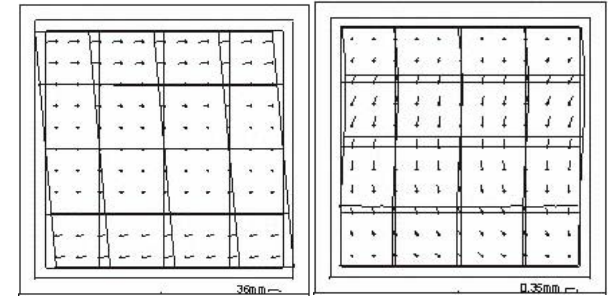


$$0 = -c \frac{a_{11}^j (Xp - Xo^j) + a_{12}^j (Yp - Yo^j) + a_{13}^j (Zp - Zo^j)}{a_{31}^j (Xp - Xo^j) + a_{32}^j (Yp - Yo^j) + a_{33}^j (Zp - Zo^j)} + \text{add param}$$

$$y = -c \frac{a_{21}^j (Xp - Xo^j) + a_{22}^j (Yp - Yo^j) + a_{23}^j (Zp - Zo^j)}{a_{31}^j (Xp - Xo^j) + a_{32}^j (Yp - Yo^j) + a_{33}^j (Zp - Zo^j)} + \text{add param}$$

$$\begin{aligned} y &= y + P1 * y & y &= y + P12 * \cos(y * 0.01600) \\ x &= x + P2 * y & x &= x + P13 * \sin(y * 0.03100) \\ x &= x + P3 * x * y & x &= x + P14 * \cos(y * 0.03100) \\ y &= y + P4 * x * y & x &= x + P15 * \sin(y * 0.01600) \\ y &= y + P5 * \sin(y * 0.12566) & x &= x + P16 * \cos(y * 0.01600) \\ y &= y + P6 * \cos(y * 0.12566) & x &= x + P17 * \sin(x * 0.11) \\ y &= y + P7 * \sin(y * 0.06283) & & * \sin(y * 0.03) \\ y &= y + P8 * \cos(y * 0.06283) & x &= x + P18 * x * y * \cos(K) \\ y &= y + P9 * \sin(y * 0.03100) & y &= y + P18 * x * y * \sin(K) \\ y &= y + P10 * \cos(y * 0.03100) & y &= y + P19 * x * y \\ y &= y + P11 * \sin(y * 0.01600) & x &= x + P20 * y * y \end{aligned}$$

ADDITIONAL PARAMETERS IMPLEMENTED IN
THE UNIVERSITY OF HANNOVER PROGRAM
BLASPO



Systematic image errors QuickBird Atlantic City, NJ
left: overall effect right: without dominating angular affinity

To avoid over-parameterization the AP are automatically eliminated using a stochastic model:

1. For each AP compute:

$$t_i = \frac{|p_i|}{\sigma_{p_i}} \quad \sigma_{p_i} = \sqrt{q_{ii}} \cdot \sigma_o, t_i \geq 1, \text{ reject if otherwise}$$

2. Compute cross-correlation coeffs. for the parameters

$$R_{ij} = \frac{q_{ij}}{\sqrt{q_{ii} q_{jj}}}; \quad R_{ij} \geq 0.85 \quad \text{Then eliminate the parameter with smaller } t_i \text{ value}$$

3. Compute $B = I - (\text{diag } N * \text{diag } N^{-1})^{-1}$; eliminate the AP that $B_{ij} > \text{or} = 0.85$



Digital Ortho. 0.5 m GSD



QB Basic Image, ~0.6 GSD

- a. GCPs Manually and automatically transferred from existing 0.5 m GSD Orthophoto**
Height of the GCPs through interpolation on a existing ± 1.3 feet Accuracy DEM (1"=1600')
Same DEM for production of Orthophoto

Type of Observations	Number of GCPs	Standard Deviation [microns]	Accuracy at GCPs		Accuracy at Check Pts	
			RMSE _x	RMSE _y	RMSE _x	RMSE _y
Manual	174	11.2	0.71	0.66		
Automatic	398	10.1	0.48	0.45		
Automatic	25	12.3	0.52	0.71	0.69	0.72
Automatic	20	13.1	0.59	0.75	0.69	0.88
Automatic	15	13.8	0.61	0.78	0.78	1.04

**Bundle Orientation with automatic selection and elimination additional parameters.
Basic QB Image. Area of Atlantic City, NJ**

- Although high attitude frequencies effects are removed at the time of basic image generation, low attitude (Yaw) effects are still present in form of affinity/angular affinity. They are effectively removed by additional parameters
- Bundle block adjustment based on properly weighted ephemeris / attitude quaternions (BBABEQ) are not enough to remove the systematic effects. Moreover, due to the narrow FOV of the HRSI, position and attitude are highly correlated making almost impossible to separate and remove their systematic effects without extending the geometric model (Self-Calib.)
- The systematic effects gets evident on the increase of accuracy (in terms of RMSE at GCPs) for looser and relaxed ground control at the expenses of large and strong block deformation with large residuals at check points. Systematic errors are more freely distributed and their effects propagated all over the block. [No functional model for SE]
- Block adjustment based on RPCs with systematic image correction functions remove significantly the affinity deformation of the basic QB images. Although relaxed ground control produces less accurate results (in terms of RMSE on GCPs) than BBABEQ, the remaining block deformations are much smaller. Increase of absolute accuracy between 65 to 80% can be reported.
- The systematic effects are also noticeable in the internal accuracy of the Block (residuals at pass/tie points). These are smaller for relaxed ground control in the BBABEQ and opposite in the case of RPCs with affine image correction function.

Further Studies need to be carried out to be more conclusive:

- 1. To conduct accuracy studies on large blocks of images with larger long overlap. This will allow a 3D accuracy study and to increase the reliability of the derived quantities.**
- 2. To extend the model of the BBABEQ to include Self-calibration making use of the co-variance matrices of the Position and Attitude to build-up proper weighting matrix.**
- 3. To include cross track image strips to study the combined effect of multi-rays points and self-calibration on the final accuracy.**
- 4. To extend the RPC model with other image correction functions, including statistical test to ensure the validity of the image correction function parameters to avoid over-parameterization.**
- 5. To test alternative orientation models such as those based on feature matching, i.e., matching of linear features existing on a land data base and extracted from the image space.**
- 6. Others**

QUESTIONS..?

ACCURACY ANALYSIS ON LARGE BLOCKS OF HIGH RESOLUTION IMAGES

Dr. Ing. Ricardo M. Passini
BAE SYSTEMS ADR

